AIP Conference Proceedings

MODELING AND EXPERIMENTS ON FAST COOLDOWN OF A 120 Hz PULSE TUBE CRYOCOOLER

Cite as: AIP Conference Proceedings **985**, 1429 (2008); https://doi.org/10.1063/1.2908503
Published Online: 27 March 2008

Srinivas Vanapalli, Michael Lewis, Gershon Grossman, et al.

MODELING AND EXPERIMENTS ON FAST COOLDOWN OF A 120 Hz PULSE TUBE CRYOCOOLER*

Srinivas Vanapalli[2,1], Michael Lewis[1], Gershon Grossman[3,1], Zhihua Gan[4,1], Ray Radebaugh[1], H.J.M. ter Brake[2]

[1]National Institute of Standards and Technology
Boulder, CO, 80305, USA.

[2]University of Twente, Postbus 217,
Enschede 7500 AE, The Netherlands.

[3]Technion-Israel Institute of Technology
Haifa, Israel 32000.

[4]Cryogenics Lab, Zheijiang University
Hangzhou, P.R. China.

ABSTRACT

High frequency operation of a pulse tube cryocooler leads to reduced regenerator volume, which results in a reduced heat capacity and a faster cooldown time. A pulse tube cryocooler operating at a frequency of 120 Hz and an average pressure of 3.5 MPa achieved a no-load temperature of 50 K. The cooling power at 80 K was about 3.35 W with a cooldown time from 285 K to 80 K of about 5.5 minutes, even though the additional thermal mass at the cold end due to flanges, screws, heater, and thermometer was 4.2 times that of the regenerator. This fast cooldown is about two to four times faster than that of typical pulse tube cryocoolers and is very attractive to many applications. In this study we measure the cooldown time to 80 K for different cold-end masses and extrapolate to zero cold-end mass. We also present an analytical model for the cooldown time for different cold-end masses and compare the results with the experiments. The model and the extrapolated experimental results indicate that with zero cold-end mass the cooldown time to 80 K with this 120 Hz pulse tube cryocooler would be about 32 s.

KEYWORDS: Cryocoolers, high frequency, pulse tube, regenerators, fast cooldown.

CP985, *Advances in Cryogenic Engineering: Transactions of the Cryogenic Engineering Conference—CEC, Vol. 53,* edited by J. G. Weisend II
© 2008 American Institute of Physics 978-0-7354-0504-2/08/$23.00

INTRODUCTION

Fast cooldown is often a desired criterion for cryocoolers. Conventionally, Joule-Thomson (JT) cryocoolers have been used to meet the requirements of fast cooldown. Open-cycle JT cryocoolers operate at very high pressure (5-8 MPa) and have a very high flow impedance at the cold end that is susceptible to clogging. Gifford-McMahon (GM), Stirling and pulse tube cryocoolers are alternatives to reach temperatures of about 50 K. Mullie et al. [1] reported improvements in cooldown time of resonant Stirling cryocoolers by matching the regenerator material heat capacity to the temperature profile that would exist at steady state in the regenerator. However, the improvements in the cooldown time were not significant. Radebaugh et al. [2] proposed a fast cooldown technique for pulse tube cryocooler that makes use of the resonance phenomenon that occurs with an appropriately sized inertance tube and reservoir volume. With a small reservoir the resonance condition can occur, which allows for higher PV power flows (higher refrigeration power). That concept applies to fast cooldown of large masses at the cold end. In this paper we discuss another method of fast cooldown that relies on high frequency and high pressure to reduce the thermal mass of the regenerator. This method is useful for applications with small cold-end masses where the regenerator heat capacity has a large influence on the cooldown time.

REFRIGERATION POWER DENSITY

For an ideal Stirling and Stirling-type pulse tube cryocooler, the cooling power is equal to the acoustic power (PV power) at the cold end and is given by

$$\dot{W}_{PV} = \tfrac{1}{2} P_1 \dot{V}_1 \cos\phi_c, \tag{1}$$

where P_1 and $\dot{V}_1$ are the amplitudes of the sinusoidal pressure and the volume flow, and ϕ_c is the phase by which the volume flow leads the pressure. The volume flow amplitude is related to the instantaneous volume amplitude V_1 at the cold end by

$$\dot{V}_1 = 2\pi f V_1. \tag{2}$$

The PV power is then given by

$$\dot{W}_{PV} = \pi f V_1 P_0 \left(\frac{P_1}{P_0} \right) \cos\phi_c, \tag{3}$$

where P_0 is the average pressure and f is the frequency. The term in parentheses is the relative pressure amplitude, which is usually not varied. From this equation we see that by increasing the frequency the PV power can be increased for fixed size of the refrigerator and operating conditions. However, simply increasing the frequency of a cryocooler designed for operating at 60 Hz would lead to higher losses because of ineffective heat transfer in the regenerator. We have shown that to efficiently operate the cryocooler at higher frequencies it is necessary to increase the average pressure and to use a regenerator matrix with a smaller hydraulic diameter [3,4]. High frequency operation of the cryocooler would also reduce the required regenerator volume. According to equation 3, for a certain PV power, increasing the frequency reduces the volume flow at the cold end for a fixed

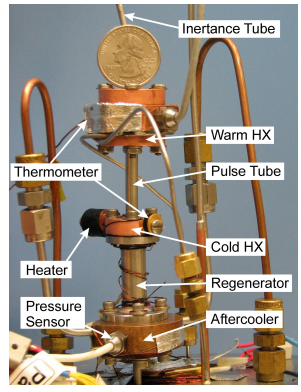

FIGURE 1. 120 Hz cryocooler showing various components. A U.S quarter (24.3 mm) is shown for size comparison

pressure ratio and phase ϕ_c. (For efficient operation, P_0 increases with frequency.) The pulse tube volume is generally chosen to be about three times the swept volume at the cold end. Reduction in swept volume due to high frequency operation of the cryocooler reduces the pulse tube volume. Hence, high frequency operation of the cryocooler reduces the volumes of the regenerator and the pulse tube for a given cooling power, which increases the power density and leads to faster cooldown.

120 Hz PULSE TUBE CRYOCOOLER

A pulse tube cryocooler was designed to operate at a frequency of 120 Hz with an average pressure of 3.5 MPa [4,5]. The flow at the cold end was made to be in phase with the pressure (ϕ_c = 0). The dimensions of various components of the cryocooler are given in table 1. Figure 1 shows the assembled cryocooler with all the instrumentation. A no-load temperature of about 50 K was achieved with a pressure ratio of 1.23 at the cold end. For an average pressure of 3.5 MPa and a pressure ratio of 1.4 at the aftercooler (1.23 at the cold end) the net refrigeration power was 3.35 W at 80 K. This cryocooler cooled from 285 K to 80 K in 5.5 minutes [4,5], but the pressure ratio or input power were not closely monitored during the cooldown. For the cooldown experiments reported here the pressure ratio at the cold end (measured at the pulse tube warm end) was held constant at 1.23 during the entire cooldown process. For comparison, one test was performed with the input power to the compressor held constant. To determine the effect of the cold-end

TABLE 1. Component geometry in pulse tube cryocooler. (All components stainless steel (SS).

	Length (mm)	**Outside Diameter (mm)**	**Wall thickness (mm)**
Regenerator	30	9.525	0.254
Pulse tube	30	4.7625	0.1524
Inertance Tube: Small dia.	864	2.3724	0.508
Large dia.	746	2.3724	0.3048
	Wire Diameter (µm)	**Porosity**	**Hydraulic Diameter (µm)**
635 Mesh (40 µm spacing)	20.3	0.601	30.6
Reservoir Volume	50 cm^3		

TABLE 2. Average heat capacities (80-285 K) of various masses at the regenerator cold end.

Cold Item	Mass (g)	Average heat capacity (J/K)
Built-in mass, M_0 (cold HX, flanges & thermometer)	26.1	9.26
Heater + screw & washer	9.2	3.10
Mass 1, M_1 (Cu)	41.7	13.88
Mass 2, M_2 (Cu)	83.9	27.93
Regenerator, (SS)	7.7	2.95

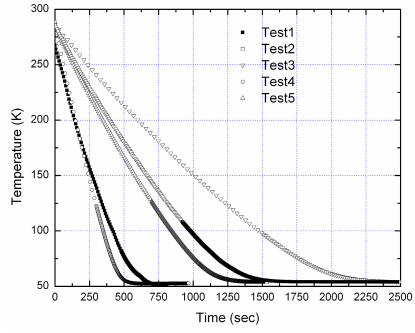

FIGURE 2 Cooldown curves under various conditions

mass on the cooling process, various copper masses were mounted at the cold end and the cooling times were recorded. The average heat capacities of the copper masses and other components are given in table 2.

EXPERIMENTAL RESULTS

Experiments were performed on the cryocooler for several cold-end masses given in table 3. For all the tests the average pressure was 3.5 MPa, the frequency was 120 Hz, and the pressure ratio was 1.23 at the cold end (measured at the warm end of the pulse tube), except for test 6 where the input power to the compressor was held constant at 275 W. Figure 2 is the plot of cooldown curves for tests 1 to 5 in table 3. The tests at constant pressure ratio were chosen to provide a constant cold-end acoustic power in order to simplify the comparison with analytical models. As shown in table 3 the cooldown time for test 6, which was performed with a constant compressor input power of 275 W, was significantly less than test 5 made with the same mass but with a constant pressure ratio. The 275 W is the steady-state input power required when the cold end is at 50 K with a pressure ratio of 1.23 at the cold end. The high input power is a result of the compressor operating far from resonance conditions at the 120 Hz frequency. A constant input power would be more realistic for cooldown during actual applications.

TABLE 3. Experimental conditions and cooldown time with various capacities. Tests 1-5 were for a constant pressure ratio of 1.23 at the warm end.

Test	Cold item	Mass (g)	Heat capacity ratio, C_r	Cooldown time, 285-80 K (s)
1	M_0 + heater	35.3	4.19	517
2	M_0 + heater + M_1	77.0	8.89	1133
3	M_0 + heater + M_2	119.2	13.66	1692
4	M_0	26.1	3.14	394
5	M_0 + M_1	67.8	7.84	970
6 (constant input power, 275 W)	M_0 + M_1	67.8	7.84	585

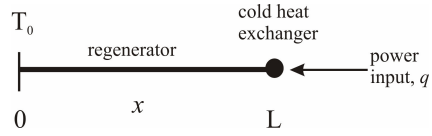

FIGURE 3. Schematic of a one-dimensional thermal model of the regenerator and the cold heat exchanger.

ANALYSIS

Analytical Model

The experimental cold stage (consisting of the regenerator, cold heat exchanger, pulse tube, warm heat exchanger) was maintained in a vacuum (<0.1 Pa), which essentially eliminates convection as a means of heat transfer. The cold stage was wrapped with several layers of multi-layer insulation, which substantially reduces the heat radiation gain from ambient. The main sources of heat transfer to the cold end are enthalpy flow, heat conduction through the regenerator material, and heat conduction through the tube walls of the regenerator and the pulse tube. To simplify the analytical model, the enthalpy flow and heat conduction were assumed to be proportional to the temperature difference between the hot and cold end for cold-end temperatures between 80 and 285 K. An effective thermal conductivity is defined as

$$k_{eff} = f_c k + k_h. \tag{4}$$

The factor f_c is the conductivity degradation factor accounting for packing of the screens [6], k_h is the simulated conduction to account for enthalpy flow, and k is the thermal conductivity of the material. The density and specific heat are taken to be independent of temperature and equal to the average value between 80 and 285 K.

The one-dimensional thermal model is illustrated in figure 3. Because of the high thermal conductivity of copper, the cold heat exchanger can be modeled as a uniform temperature thermal mass with a total heat capacity C_M. The warm-end heat sink is assumed to be at a constant temperature T_0 and the heat flows by the effective thermal conductivity given in eq. (4) through the regenerator, simulating conduction through a solid rod of the same solid cross-sectional area. If the temperature of the regenerator and the cold heat exchanger were initially at the heat sink temperature T_0 and a step power q is applied ($q < 0$ for refrigeration) at the cold heat exchanger at $t>0$, the cold heat exchanger temperature T is given by [7,8],

$$T(t) = T_0 + \frac{qL}{k_{eff} A_c}\left[1 - \sum_{n=1}^{\infty} \frac{4\sin^2 \xi_n}{\xi_n (2\xi_n + \sin 2\xi_n)} \exp(-\frac{t}{\tau_n})\right] \tag{5}$$

where A_c is the solid cross-sectional area, L is the regenerator length, and the time constants are

$$\tau_n = \rho c_p L^2 / k_{eff} \xi_n^2 , \tag{6}$$

where ρ is the solid density, c_p is the specific heat of the regenerator matrix and the eigenvalues ξ_n are determined by the positive solutions to the equation

$$\xi_n \tan \xi_n = \frac{\rho A_c L c_p}{C_M} = \frac{1}{C_r}. \quad (7)$$

where C_M is the heat capacity of the cold-end mass and C_r is the heat capacity ratio between the cold-end mass and the regenerator mass. When C_M approaches zero the result gives the intrinsic cooldown time when there is no cold-end mass. For the intrinsic case of zero cold-end mass we derived an alternative analytical model that gives the temperature as a function of both time and position x between the warm and cold ends. The result is given by

$$T(x,t) = T_0 + \frac{qx}{k_{eff} A_c} - \sum_{n=1}^{\infty} A_n \sin\left[\frac{(2n-1)\pi x}{2L}\right] \exp\left(-\frac{t}{\tau_n^*}\right), \quad (8)$$

where the constants are,

$$A_n = \frac{8qL\sin[(2n-1)\pi/2]}{k_{eff} A_c \pi^2 (2n-1)^2} = \frac{8qL(-1)^{n+1}}{k_{eff} A_c \pi^2 (2n-1)^2}, \tau_n^* = 4L^2/\pi^2 (2n-1)^2 \alpha_m, \alpha_m = k_{eff}/\rho c_p \quad (9)$$

Equation (8) is similar to the equation derived by Reese and Tucker [9] for use in measuring specific heats, except for a small error in their published equation. Note that in our case q<0. The analytical equations rely on the use of the effective thermal conductivity given by eq. (4) that takes into account the enthalpy flow in the regenerator. We rely on a numerical model described in next section to calculate this enthalpy flow loss.

Numerical Analysis

The NIST numerical model, known as REGEN3.2 and based on finite difference equations for the conservation equations, was used for the calculations discussed here. In REGEN3.2 the mass flow at the cold end and its phase with respect to the pressure at the cold end are input parameters, along with the desired average pressure, pressure ratio, frequency, and the geometrical parameters of the regenerator matrix. The mass flow at the warm end (both magnitude and phase) is calculated by the model. Losses associated with regenerator ineffectiveness, conduction through the matrix, and pressure drop are calculated by the model. Conduction loss through the tube containing the screen matrix is calculated separately. A loss associated with the expansion process (pulse tube) was taken to be 20 % of the gross refrigeration power.

The enthalpy flow loss in the regenerator is not linear with the temperature difference between the two ends of the regenerator. The enthalpy flow tends to increase rather rapidly as the cold end cools below about 100 K, which for a constant input PV power causes the net refrigeration power to decrease rapidly below 100 K. To estimate the net cooling power as a function of cold end temperature, REGEN runs were performed with the dimensions of the regenerator given in table 1 with varying cold end temperatures. The average pressure of 3.5 MPa, a pressure ratio of 1.23 at the cold end and a frequency of 120 Hz were taken to match with the experimental data. The flow at the cold end was made to be in phase with the pressure (ϕ_c = 0) for all the runs. Since the mass flow is a function of temperature, the mass flow for various runs was adjusted from the mass flow value of 1.9 g/s at 80 K. The warm end temperature was taken to be 300 K.

Heat conduction loss through the pulse tube and regenerator walls as well as a radiation heat loss of about 0.06 W were subtracted from the net cooling power calculated by REGEN3.2. Figure 4 is the plot of the adjusted gross refrigeration power (gross minus the 20 % pulse tube loss), net refrigeration power, input PV power and heat loss as a function of temperature. The heat loss takes into account the enthalpy flow as well as the conduction and radiation losses. The adjusted gross refrigeration power was about 8.17 W. The heat loss was approximated by a straight line between 300 K and 80 K, and the effective thermal conductance was found to be 0.014 W/K. The equivalent conductivity due to enthalpy flow in eq. (4) was adjusted to yield this effective thermal conductance. The appropriate enthalpy factor was found to be $k_h / f_c k = 10.27$, with f_c = 0.13, and k = 11.32 W/(m·K). This effective thermal conductivity from equation (4) was then used in the analytical equations for the cooldown time.

COMPARISON OF EXPERIMENTAL AND CALCULATED RESULTS

Figure 4 also shows the measured net refrigeration power as compared with that calculated by REGEN3.2. We see that the experimental values in the range between 80 and 100 K are close to, but slightly less than, the calculated values. That could indicate the pulse tube ineffectiveness may be slightly larger than 20 %, thereby reducing the adjusted gross refrigeration power. If we maintain the enthalpy factor at 10.27 and use a single adjusted gross refrigeration power q (equal to $\dot{Q}_{gross,adj}$ in figure 4) in eq. (5) to give the best agreement between the calculated cooldown times and the experimental results, we find q to be -6.63 W (minus indicates refrigeration) instead of -8.17 W from REGEN3.2. The dashed curve in figure 5 represents the cooldown times calculated from eq. (5) with q = -6.63 W. When q = -6.63 W is used in eq. (5) or (8) for the intrinsic cooldown time from 285 K to 80 K a value of 31.5 s is obtained. The experimental data are also shown in Figure 5 for comparison. The solid line is a least squares linear fit to the experimental data. That fit extrapolates to a cooldown time from 285 K to 80 K of 29.7 ± 59.7 s for zero cold-end mass. In practice a small but finite cold-end mass is required to accommodate a heat exchanger, a small thermometer, and some device to be cooled. Heat capacity ratios C_r less than 1.0 would be reasonable in some applications. The major uncertainty in the experimental results is that of the built-in cold-end mass, M_0. Small variations in the pressure ratio during cooldown result in an uncertainty for the experimental cooldown times of about 5 %.

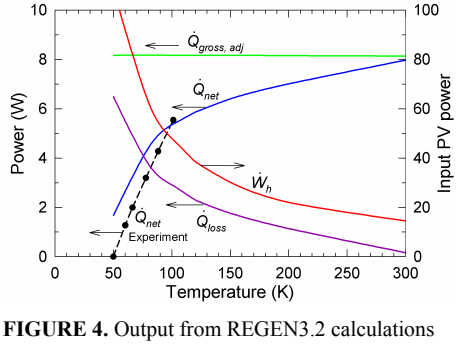

FIGURE 4. Output from REGEN3.2 calculations compared with experimental results.

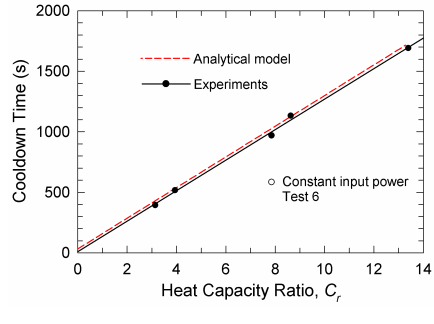

FIGURE 5. Measured and calculated cooldown times for various ratios of cold-end heat capacity to regenerator heat capacity

CONCLUSION

We have shown that increasing the frequency and average pressure in an optimized pulse tube cryocooler leads to shorter cooldown times. A pulse tube cryocooler with a significant cold-end mass operating at 120 Hz and 3.5 MPa average pressure was shown to cool from 285 K to 80 K in 5.5 minutes. Cooldown times for various cold-end masses attached to this cryocooler were measured under the condition of a constant cold end pressure ratio of 1.23. A linear extrapolation of these times to zero cold-end mass showed a cooldown time to 80 K of about 29.7 ± 59.7 s, which agrees within experimental error with the value of 31.5 s found by the use of an analytical model.

ACKNOWLEDGEMENT

The authors acknowledge Mike Rybowiak for careful machining of the parts. One of the authors (S.V) was supported by STW (Dutch Technology Foundation) "3LN Microcooler" (TTF.5677).

REFERENCES

1. Mullie, J., Groep, vd Willem., Bruins, P., Benschop, T., Koning, de A., Dam, J., "Improvement of cooldown time of LSF 9599 flexure bearing sada cooler", 2006, SPIE.
2. Radebaugh, R., O'Gallagher, A., Lewis, M. A., and Bradley, P. E., "Proposed rapid cooldown technique for pulse tube cryocoolers," in *Cryocoolers 14, edited by S.D. Miller and R.G. Ross, Jr.*, 2007, pp. 231-240.
3. Radebaugh, R. and O'Gallagher, A., "Regenerator operation at very high frequencies for microcryocoolers," in *Advances in Cryogenic Engineering*, vol. 51, 072504, American Institute of Physics, 2006, pp. 1919-1928.
4. Vanapalli, S., Lewis, M., Gan, Z., and Radebaugh, R., "120 Hz pulse tube cryocooler for fast cooldown to 50 K", in *Applied Physics Letters,* vol. 90, No. 7, American Institute of Physics, 2007.
5. Vanapalli, S., Lewis, M., Gan, Z., Bradley, P., and Radebaugh, R., "Modelling and experiments of a 120 Hz pulse tube cryocooler operating at 50 K with fast cooldown," to be published in *Cryogenics*.
6. Lewis, M. A. and Radebaugh, R., "Measurement of heat conduction through bonded regenerator matrix materials," in *Cryocoolers 12*, edited by R.G. ross, Jr., 2003, pp. 517-522.
7. Zhang, Z. M., Lorentz, S. R., Rice, J. P., and Datla, R. U., "Measurement of thermophysical properties of polyimide and a black paint for future development of cryogenic radiometers," in *Metrologia,* vol. 35, 1998, pp. 511-515.
8. Johnson, B. C., Kumar, A. R., and Zhang, Z. M., "Heat transfer analysis and modeling of a cryogenic laser radiometer," in *J. Thermophysics and Heat Transfer*, vol. 12, No. 4, 1998, pp. 575-581.
9. Reese, W., and Tucker, J. E., "Thermal conductivity and specific heat of some polymers between 4.5 K and 1 K," in *J. Chem. Phys.,* Vol. 43, No. 1, 1965, pp. 105-114.